

# NON-LINEAR DYNAMICS OF LAMINATED PLATES WITH A HIGHER-ORDER THEORY AND $C^0$ FINITE ELEMENTS

T. KANT and MALLIKARJUNA

Department of Civil Engineering, Indian Institute of Technology, Powai, Bombay 400076, India

(Received 15 September 1989; in revised form 24 April 1990)

**Abstract**—Impact responses of composite laminates are investigated with  $C^0$  finite elements. A nine-node isoparametric quadrilateral element based on a higher-order theory and the von Kármán large deflection assumptions is developed. An experimentally established contact law which accounts for the permanent indentation is incorporated into the finite element program to evaluate the impact force. In the time integration, the explicit central difference technique is used in conjunction with the special mass matrix diagonalization scheme. Numerical results, including the contact force histories, deflections and strains in the plate, are presented.

## 1. INTRODUCTION

In many engineering applications, laminated fibre-reinforced composite structures are subjected to central impact loading of a small cylindrically shaped blunt-ended projectile. An understanding of the transient behaviour of composite laminates under this type of loading is therefore essential. Most of the impact problems have been formulated using the small deflection theory [1] which is adequate if the impact load is small. Shivakumar *et al.* [2] have developed a stress analysis method to include the effects of geometric non-linearity under quasi-static conditions. The linear [3, 4] and non-linear [5-9] transient analysis of composite plates has not received much attention as evidenced by the few publications.

A generalization of the von Kármán [10] non-linear plate theory for isotropic plates to include the effects of transverse shear and rotary inertia in the theory of orthotropic plates is due to Medwadowski [11] and that for anisotropic plates is due to Ebcioğlu [12]. Recently, Reddy *et al.* [13-16] and the present authors [17-20] emphasized the credibility of high-order shear deformable theories for dynamics of anisotropic laminates. In this paper, dynamic large deflection response of laminated composite plates impacted by a hard object is investigated using a refined theory with  $C^0$  element. In order to calculate the contact force, an experimentally established contact law which accounts for the permanent indentation is employed.

## 2. NON-LINEAR THEORY OF ANISOTROPIC LAMINATES

Consider a composite laminate consisting of thin homogeneous orthotropic layers, oriented arbitrarily and having a total thickness  $h$ . Let the  $x$ - $y$  plane coincide with the middle plane of the laminate with the  $z$ -axis oriented in the thickness direction. In the present theory, the displacement components of a generic point in the laminate are assumed to be of the form [7, 13].

$$\begin{aligned}u(x, y, z, t) &= u_0(x, y, t) + z\theta_x(x, y, t) + z^3\theta_x^*(x, y, t) \\v(x, y, z, t) &= v_0(x, y, t) + z\theta_y(x, y, t) + z^3\theta_y^*(x, y, t) \\w(x, y, z, t) &= w_0(x, y, t)\end{aligned}\tag{1}$$

where  $t$  denotes time;  $u_0$ ,  $v_0$ , and  $w_0$  are mid-plane displacements of a generic point having displacements  $u$ ,  $v$ , and  $w$  in the  $x$ ,  $y$ , and  $z$  directions respectively;  $\theta_x$  and  $\theta_y$  are rotations of the transverse normal cross-sections in the  $xz$  and  $yz$  planes, respectively;  $\theta_x^*$  and  $\theta_y^*$  are the corresponding higher-order terms in the Taylor's series expansion. A Lagrangian approach

Contributed by J. N. Reddy.

is adopted and the stress and strain descriptions used are those due to Piola–Kirchhoff, and Green, respectively. For geometric non-linearity alone (large elastic displacements and rotations but subject to small strain assumptions) considered here, the stress–strain relationship is in terms of the total values. Both isotropic and anisotropic situations can be accommodated. By invoking the von Kármán large deflection assumptions, we have the following Green–Lagrange strain–displacement relations:

$$\begin{aligned}\varepsilon_x &= \frac{\partial u}{\partial x} + \frac{1}{2} \left( \frac{\partial w}{\partial x} \right)^2 \\ \varepsilon_y &= \frac{\partial v}{\partial y} + \frac{1}{2} \left( \frac{\partial w}{\partial y} \right)^2 \\ \gamma_{xy} &= \frac{\partial u}{\partial y} + \frac{\partial v}{\partial x} + \frac{\partial w}{\partial x} \frac{\partial w}{\partial y} \\ \gamma_{yz} &= \frac{\partial v}{\partial z} + \frac{\partial w}{\partial y} \\ \gamma_{zx} &= \frac{\partial u}{\partial z} + \frac{\partial w}{\partial x}.\end{aligned}\quad (2)$$

To develop the finite element equations of motion of a composite plate impacted by a mass, we consider a system consisting of the plate and the impactor. We assume that the equilibrium configurations of the system from time 0 to time  $t$  have been obtained. Under the assumptions of small strain and conservative loading, the virtual equation for the system at time  $t + \Delta t$  is written in a Lagrangian coordinate system as follows:

$$\int_{A_0} \delta \mathbf{d}^T M \ddot{\mathbf{d}} dA + \int_{A_0} \delta \bar{\mathbf{e}}^T \bar{\boldsymbol{\sigma}} dA + \delta w_s m_s \ddot{w}_s + F \delta \alpha = 0 \quad (3a)$$

where;  $A_0$  is the undeformed plate area;  $\mathbf{d}^T$  are the generalized displacements  $u_0, v_0, w_0, \theta_x, \theta_y, \theta_x^*, \theta_y^*$ ;  $M$  is the laminate mass matrix;  $\bar{\mathbf{e}}$  are the laminate mid-plane strains [18–20];  $\bar{\boldsymbol{\sigma}}$  are the laminate mid-plane stress-resultants [18–20];  $\delta$  denotes variation;  $m_s, w_s$  and  $\ddot{w}_s$  are the mass, displacement and acceleration of the impactor, respectively;  $F$  is the contact force between the plate and the impactor; and  $\alpha$  is the indentation given by

$$\alpha = w_s(t + \Delta t) - w_0(x_0, y_0, t + \Delta t) \quad (3b)$$

in which  $w_0$  is the plate deflection at the impact point  $(x_0, y_0)$ . It should be noted that the quantities  $\mathbf{d}, \bar{\mathbf{e}}, \bar{\boldsymbol{\sigma}}, w_s, F$  and  $\alpha$  in equation (3) are presented at time  $t + \Delta t$ .

The laminate constitutive relations are obtained as,

$$\begin{Bmatrix} \mathbf{N} \\ \mathbf{M} \\ \mathbf{M}^* \\ \mathbf{Q} \\ \mathbf{Q}^* \end{Bmatrix} = \begin{bmatrix} \mathbf{D}_m & \mathbf{D}_c & \mathbf{0} \\ \mathbf{D}_c^T & \mathbf{D}_b & \mathbf{0} \\ \mathbf{0} & \mathbf{0} & \mathbf{D}_s \end{bmatrix} \begin{Bmatrix} \bar{\mathbf{e}}_p \\ \bar{\mathbf{e}}_b \\ \bar{\mathbf{e}}_s \end{Bmatrix} + \begin{Bmatrix} \bar{\mathbf{e}}_L \\ \mathbf{0} \\ \mathbf{0} \end{Bmatrix} \quad (4)$$

or symbolically,

$$\bar{\boldsymbol{\sigma}} = \mathbf{D}(\bar{\mathbf{e}}_0 + \bar{\mathbf{e}}_L) = \mathbf{D} \bar{\mathbf{e}}. \quad (5)$$

In equations (4) and (5),  $N_i, (M_i, M_i^*)$  and  $(Q_i, Q_i^*)$  are the in-plane stress resultants, stress moments, and transverse shear forces, respectively. The coefficients  $D_{m_{ij}}, D_{c_{ij}}, D_{b_{ij}}$  and  $D_{s_{ij}}$  are the respective in-plane, bending in-plane (coupling), bending, and transverse shear stiffnesses, and  $\bar{\mathbf{e}}_0$  and  $\bar{\mathbf{e}}_L$  are the generalized linear and non-linear strains, respectively [7].

### 3. C<sup>0</sup> FINITE ELEMENT FORMULATION

The finite element used here is a nine-node isoparametric quadrilateral element. The laminate displacement field in the element can be expressed in terms of the nodal variables

as

$$\mathbf{d}(\xi, \eta, t) = \sum_{i=1}^{NN} N_i(\xi, \eta) \mathbf{d}_i(t) \quad (6)$$

where  $NN$  is the number of nodes in an element,  $N_i(\xi, \eta)$  contains the interpolation functions associated with node  $i$  in terms of the normalized coordinates  $\xi$  and  $\eta$ ,  $\mathbf{d}_i(t)$  is the generalized displacement vector corresponding to  $i$ th node of an element. The generalized Green strain vector  $\bar{\epsilon}$  given by equation (5) in terms of nodal displacements  $\mathbf{a}$ , displacement gradients  $\mathbf{A}_0$ , Cartesian derivatives of shape function matrix  $\mathbf{N}$  and their variations  $\delta\bar{\epsilon}$  are written in the form,

$$\bar{\epsilon} = (\mathbf{B}_0 + \frac{1}{2} \mathbf{B}_L) \mathbf{a} \quad (7a)$$

$$\delta\bar{\epsilon} = (\mathbf{B}_0 + \mathbf{B}_L) \delta\mathbf{a} \quad (7b)$$

where  $\mathbf{B}_0$  is the strain matrix giving the linear strains,  $\mathbf{B}_L$ , which is linearly dependent upon  $\mathbf{a}$ , gives the non-linear strain. Consequently the non-linear strains are quadratically dependent upon the nodal displacements  $\mathbf{a}$ , where

$$\mathbf{a} = [d_1^T, d_2^T, \dots, d_{NN}^T]^T. \quad (7c)$$

Substituting equations (6) and (7) into (3a) and considering  $\delta\mathbf{a}$  and  $\delta w_s$  to be arbitrary, equation (3a) can be partitioned into two sets of equations

$$m_s \ddot{w}_s + F = 0 \quad (8)$$

and

$$M\ddot{\mathbf{a}} + K_0 \mathbf{a} + H(\mathbf{a}) \mathbf{a} = \mathbf{F} \quad (9)$$

where  $M$  is the mass matrix,  $K_0$  is the linear elastic stiffness matrix,  $\mathbf{F}$  is the contact force vector, and  $H(\mathbf{a})$  is the generalized non-linear stiffness matrix which is given by

$$H(\mathbf{a}) = \int_{A_0} \mathbf{B}_0^T \bar{\sigma}_L dA + \int_{A_0} \mathbf{B}_L^T \bar{\sigma} dA. \quad (10)$$

In equation (10),  $\bar{\sigma}_L$  are the stresses induced by the non-linear part of the strain. It should be noted that the contact force vector  $\mathbf{F}$  must be calculated before the plate motion can be analysed using equation (9).

In an initially stressed flat plate, equation (9) should be rewritten as [9],

$$M\ddot{\mathbf{a}} + (K_0 + K_\sigma) \mathbf{a} + H(\mathbf{a}) \mathbf{a} = \mathbf{F} \quad (11)$$

in which  $K_\sigma$  is the so-called initial stress stiffness matrix.

#### 4. SPECIAL MASS MATRIX DIAGONALIZATION SCHEME

The inertia force vector requires the evaluation of the mass matrix  $M$ . This consistent mass matrix is not diagonal and it must therefore be diagonalized in some way if it is to be useful in the explicit marching scheme. For the quadratic isoparametric elements used here, several alternatives were investigated by Hinton *et al.* [21]. The most efficient scheme found to date can be summarized as follows:

(i) Only the diagonal coefficients of the consistent mass matrix are computed.

$$M = \int_A \mathbf{N}^T \bar{\mathbf{m}} \mathbf{N} dA \quad (12a)$$

where

$$\bar{\mathbf{m}} = \begin{bmatrix} I_1 & & & & & & 0 \\ & I_1 & & & & & \\ & & I_1 & & & & \\ & & & I_2 & & & \\ & & & & I_2 & & \\ & & & & & I_3 & \\ 0 & & & & & & I_3 \end{bmatrix} \quad (12b)$$

in which  $I_1$ ,  $I_2$  and  $I_3$  are normal inertia, rotary inertia and higher-order inertia terms, respectively. These are given by

$$(I_1, I_2, I_3) = \sum_{L=1}^{NN} \int_{h_{L-1}}^{h_L} (i, z^2, z^6) \rho^L dz \quad (12c)$$

and  $\rho^L$  is the material density of the  $L$ th layer.

(ii) The total mass of the element is computed,

$$M_i = \int_{\text{vol}} \rho d(\text{vol}). \quad (13)$$

(iii) The diagonal coefficients  $M_{ii}$  associated with translation (but not rotation) degrees of freedom, are summed such that

$$\text{SUM} = \sum M_{ii} \quad (14)$$

(iv) All the diagonal coefficients of the consistent mass matrix are scaled in the following manner.

$$M_{ii}^d = M_{ii} \frac{M_i}{\text{SUM}}. \quad (15)$$

## 5. INDENTATION LAW

When a composite laminate is impacted by a mass, contact force results. This contact force must be calculated before the plate motion can be analysed using equations (9) or (11). The evaluation of the contact force depends on a contact law which relates contact force with indentation. Recently, Yang and Sun [22] have proposed a power law based on static indentation tests using steel balls as indentors. This contact law accounts for permanent indentation after unloading cycles. The modified version which was obtained by Tan and Sun [23] is used in the present study.

In ref. [23], a 20-plyed  $(0^\circ/45^\circ/0^\circ/-45^\circ/0^\circ)_2s$  graphite/epoxy laminate with a thickness of 0.269 cm and two spherical steel indentors with diameters of 1.27 and 1.905 cm were used in the indentation test.

The contact law is given as follows:

$$\text{loading: } F = K \alpha^{1.5} \quad 0 < \alpha \leq \alpha_m \quad (16)$$

$$\text{unloading: } F = F_m \left( \frac{\alpha - \alpha_0}{\alpha_m - \alpha_0} \right)^q \quad (17)$$

$$\text{reloading: } F = F_m \left( \frac{\alpha - \alpha_0}{\alpha_m - \alpha_0} \right)^{1.5}. \quad (18)$$

In the above equations,  $\alpha_m$  is the maximum indentation during loading,  $F_m$  is the maximum contact force at the beginning of unloading,  $\alpha_0$  denotes the permanent indentation in a loading-unloading cycle and is given by

$$\alpha_0 = \begin{cases} \beta(\alpha_m - \alpha_p) & \text{if } \alpha_m > \alpha_p \\ 0 & \text{if } \alpha_m < \alpha_p \end{cases} \quad (19)$$

in which constants  $\beta$  and  $\alpha_p$  were found to be 0.094 and  $1.667 \times 10^{-2}$  cm, respectively. For the indenter of 1.27 cm diameter, the contact coefficient  $K$  and power index of the unloading law were found to be  $1.413 \times 10^6$  N/cm<sup>1.5</sup> and 2.5, respectively.

The contact law given by equations (16)–(18) is incorporated into (8) and (11) to solve for the impact response.

## 6. SOLUTION ALGORITHM

It is well known that a considerable computational effort is needed in non-linear transient analysis of structures. In the present work, the very popular and easily implemented, explicit

central difference scheme is used which is discussed elsewhere [7, 24]. During each time step, relatively little computational effort is required, since no stiffness and mass matrices of the complete element assemblage need to be formed, the solution can essentially be carried out on the element level and relatively little high-speed storage is required. Using this scheme, systems of very large order can be solved effectively. Unfortunately the method is conditionally stable and very small time steps are often needed. Therefore the computational advantages of the central difference scheme are counterbalanced by the very small size of time step necessary when some stiff and/or small elements are present.

In the present investigation, after carrying out the extensive numerical computations [7], the empirical relation given by Tsui and Tong [25] is modified. The following empirical relation is suggested to estimate the critical time step length for the transient response of anisotropic composite laminates. That is,

$$\Delta t \leq \Delta t_{cr} = \Delta x \left[ \frac{\rho(1 - \nu^2)}{E_2 R \{ 2 + (1 - \nu)(\pi^2/12)(1 + 1.5(\Delta x/h)^2) \}} \right]^{1/2} \quad (20)$$

in which  $R = E_1/E_2$ ,  $\Delta x$  is the smallest distance between adjacent nodes in any quadrilateral element used.  $E_1$  and  $E_2$  are the Young's moduli, where subscript 1 refers to the direction of fibres and 2 refers to the transverse direction.

In the numerical evaluation for the stiffness and mass matrices, and the force vector, the so-called selective-reduced integration is employed. A  $3 \times 3$  Gaussian rule is used to compute the inertia terms and in-plane, coupling between inplane and bending, bending deformations while a reduced  $2 \times 2$  rule is used to evaluate the terms associated with transverse shear deformation. It should be noted that the contact force vector has to be computed before the next iteration is carried out.

## 6. RESULTS AND DISCUSSION

In order to demonstrate the versatility of the refined theory and  $C^0$  finite element developed, several examples drawn from the literature are evaluated and discussed. Computer programs have been developed for the higher order shear-deformation theory (HOST) with five degrees of freedom ( $w_0, \theta_x, \theta_y, \theta_x^*, \theta_y^*$ ) and seven degrees of freedom ( $u_0, v_0, w_0, \theta_x, \theta_y, \theta_x^*, \theta_y^*$ ) for linear (HOST5) and non-linear (NLHOST7) analyses, respectively. In addition to the HOST, programs were developed for first order shear-deformation theory (FOST) with three degrees of freedom ( $w_0, \theta_x, \theta_y$ ) and five degrees of freedom ( $u_0, v_0, w_0, \theta_x, \theta_y$ ) for linear (FOST3) and non-linear (NLFOST5) analyses, respectively. All computations were carried out in single precision on CDC CYBER 180/840 computer at the Indian Institute of Technology, Bombay, India.

Firstly, an example, which was solved by Akay [26] using a four-node isoparametric quadrilateral mixed finite elements with a  $2 \times 2$  mesh in a quadrant of an isotropic square plate and a time increment of  $\Delta t = 0.005$  s is considered here. In the present study, only one element in a quadrant is used. The boundary conditions are assumed to be simply-supported and the plate is subjected to a uniform pulse load of magnitude  $q$ . A thin plate with the following parameters [26] is considered:

$$a = 243.8 \text{ cm}, \quad h = 0.635 \text{ cm}, \quad \nu = 0.25$$

$$E = 7.031 \times 10^5 \text{ kg/cm}^2, \quad \rho = 2.547 \times 10^{-6} \text{ kg s}^2/\text{cm}^4$$

$$q(x, y, t) = 4.882 \times 10^{-4} \text{ kg/cm}^2, \quad 0 \leq t < \infty.$$

The same plate with the same material properties was analysed also by Bayles *et al.* [27] who developed a finite difference scheme for dynamic von Kármán equations, and employed an  $8 \times 8$  mesh and a time increment of  $\Delta t = 0.0005$  s. A trigonometric solution of the same problem is due to Yamaki [28].

The vibration of centre transverse deflection with respect to time for different load magnitudes  $q, 5q$  and  $10q$ , is shown in Fig. 1(a). The variation of maximum (peak) centre deflection and bending moment with respect to different load magnitudes is shown in Fig. 1(b). The results obtained by using NLFOST5, HOST3 and HOST5 are also presented in Fig. 1(a) and (b) for comparison purposes. The effect of load magnitude on non-linear

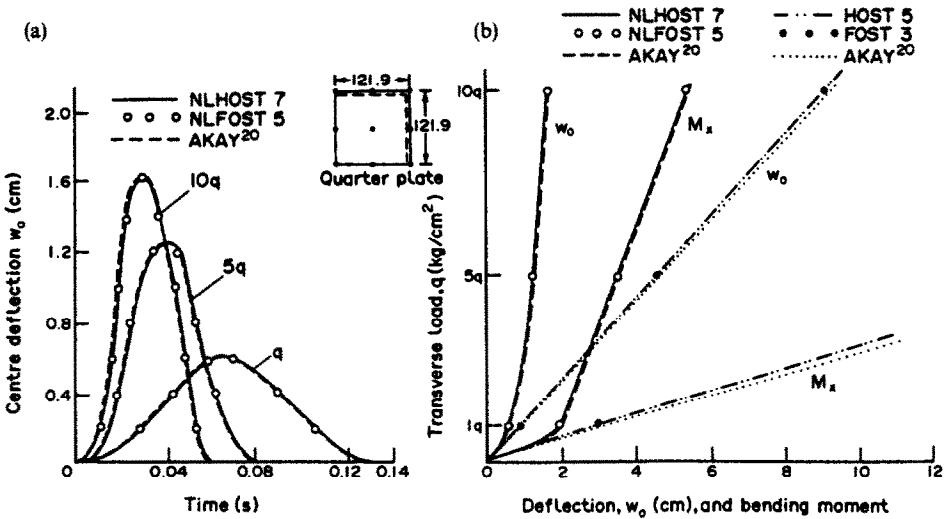


Fig. 1. Non-linear transient response of isotropic square plate under suddenly applied uniformly distributed pulse loading ( $a = b = 243.8$  cm,  $h = 0.635$  cm,  $q = 4.882 \times 10^{-4}$  kg/cm<sup>2</sup>,  $\Delta t = 0.1 \times 10^{-5}$  s, quarter plate with one element). (a) Variation of transverse deflection with time. (b) Variation of maximum centre deflection and bending moment with different load magnitudes.

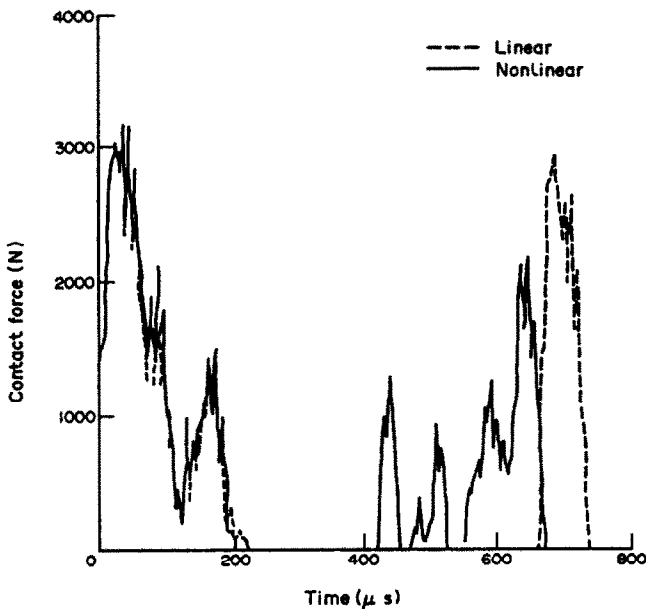


Fig. 2. Comparison of contact forces using the linear and non-linear plate theories.

response is clearly seen in these plates. It is observed that the nine-noded quadrilateral isoparametric element is capable of rendering good accuracy with relatively coarse mesh. The decrease in magnitude of the peak deflection and moment as predicted by the non-linear theory are of interest. The effect of the non-linearity (von Kármán type) is to decrease the amplitude and period of the centre deflection, and the stress-resultants.

Next, the parametric effects of time step, mesh size, aspect ratio, side-to-thickness ratio, lamination scheme and material anisotropy on dynamic response of the laminated composites have been studied [7]. In view of this finding, the  $8 \times 8$  mesh is used to model the whole plate in the following analysis. The laminated composite plate considered is a 20-ply  $[0^\circ/45^\circ/0^\circ/-45^\circ/0^\circ]_{25}$  laminate with dimension  $15.24 \times 10.16 \times 0.269$  cm. The plate is assumed to be impacted at the centre by a steel impactor with a contacting spherical cap of diameter 1.27 cm. The boundary conditions are simply supported and immovable in the

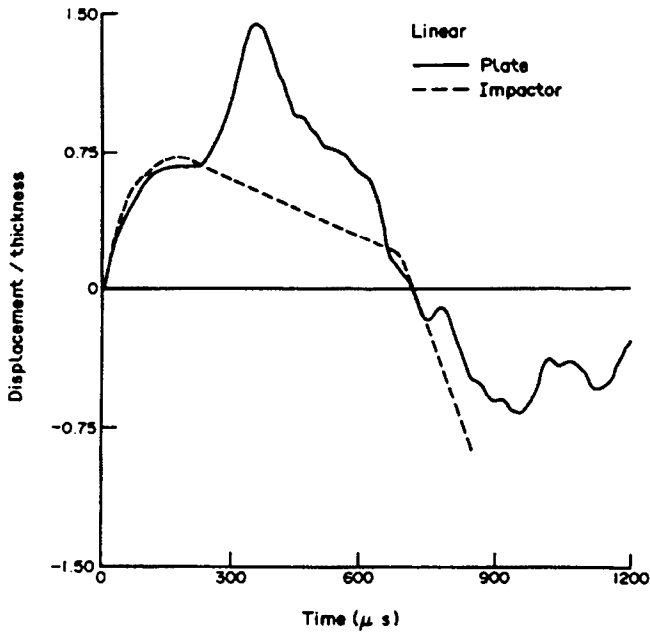


Fig. 3. Motions of the plate and the impactor using the linear plate theory.

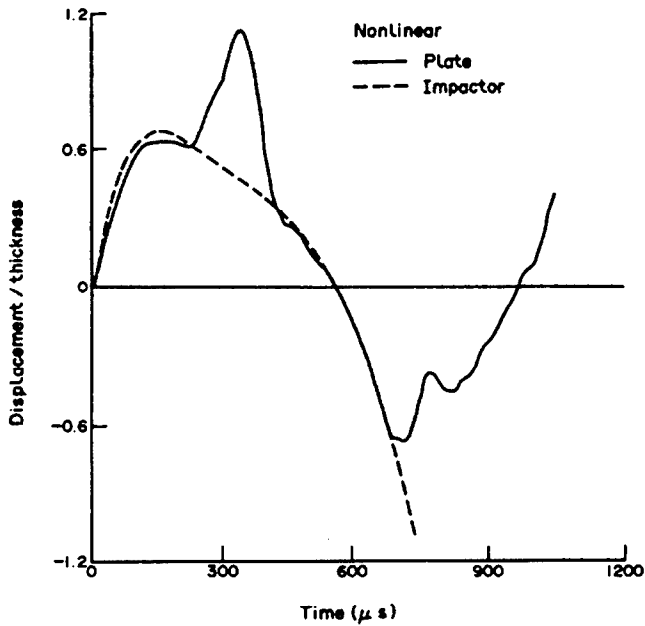


Fig. 4. Motions of the plate and the impactor using the non-linear plate theory.

planes of the plates along all the edges. The elastic properties of a graphite/epoxy lamina are assumed to be,

$$\begin{aligned}
 E_1 &= 120 \text{ GPa,} & E_2 &= 7.9 \text{ GPa} \\
 \nu_{12} &= 0.3, & G_{12} &= G_{23} = G_{13} = 5.5 \text{ GPa} \\
 \rho &= 1.58 \times 10^{-5} \text{ N s}^2/\text{cm}^4.
 \end{aligned}$$

The motion of the impactor is along the positive  $z$ -direction. The laminate is impacted by an impactor of mass  $8.537 \times 10^{-5} \text{ N s}^2/\text{cm}$  with an initial impact velocity of 30 m/s. Figure 2 presents the comparison of the contact force histories using the small deflection theory and

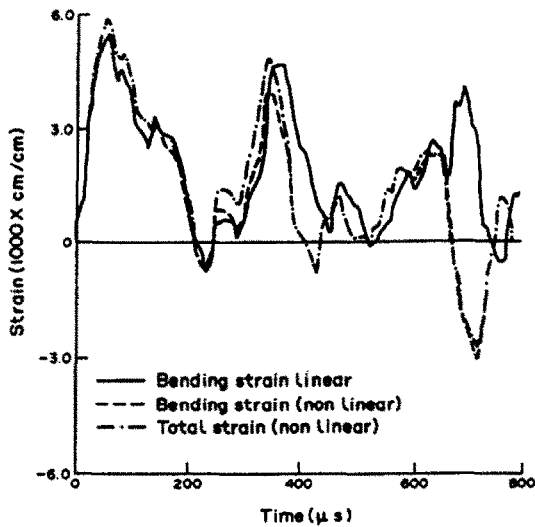


Fig. 5. Comparison of the extreme strain  $\epsilon_{xx}$  using linear and non-linear plate theories.

the large deflection theory. The time increments chosen are  $0.25 \mu\text{s}$  for the latter and  $0.5 \mu\text{s}$  for the former. It is seen that there does not exist significant differences between the contact forces in the first contact duration. However, there are four contacts according to the large deflection theory. It is also of interest to note that the maximum value of the contact force in the second contact for the small deflection theory is larger than any of the secondary contacts for the large deflection theory.

Figures 3 and 4 show the relative motions of the plate and the impactor for both the theories. A reduction of the peak deflection is noted. The histories of the strains  $\epsilon_{xx}$  at the Gaussian point (0.2147, 0.1431 cm) on the surface which is opposite to the impact surface are presented in Fig. 5. It should be noted that the maximum strains do not occur at the same time as do the maximum deflections. Also there exists insignificant difference among these extreme strains during the first contact. This can be explained by the fact that the deflection during this period is very small and the effect of geometrical non-linearity is negligible.

From Fig. 5, we also note that the bending strain according to the large deflection theory is smaller than that of the linear theory. However, the total strain (bending plus membrane strain) is larger than that in the linear case. It should be noted that the opposite conclusion is obtained for the strains at the opposite surface.

## 7. CONCLUSION

A refined shear flexible finite element including the effect of geometric non-linearity is employed in the impact analysis of laminated composite plates. Comparisons of the contact force histories, deflections and strains in the plate using both the small deflection theory and the large-deflection theory are presented. The numerical results clearly show that the large deflection theory predicts smaller deflections. The advantage in the use of a higher-order theory presented here over the Mindlin theory hitherto used is not quite evident for the isotropic plates. But such an usage is very effective in the analysis of nonhomogeneous, anisotropic, composite-sandwich structures, and relatively thicker plates as the mathematical model on which this theory based is far superior to the Reissner/Mindlin theory.

*Acknowledgement*—Partial support of this research by the Aeronautics Research and Development Board, Ministry of Defence, Government of India through its Grant Nos Aero/RD-134/100/84-85/362 and Aero/RD-134/100/88-89/518 is gratefully acknowledged.



## REFERENCES

1. H. Aggour and C. T. Sun, Finite element analysis of a laminated composite plate subjected to circularly distributed central impact loading. *Comput. Struct.* **28**, 729–36 (1988).
2. K. N. Shivakumar, W. Elber and W. Illg, Analysis of progressive damage in thin circular laminates due to static-equivalent impact loads. 24th AIAA/ASME/AHS Structure, Structural Dynamics, and Material Conf., Lake Tahoe, Nevada (May 1983).
3. J. N. Reddy, Dynamic (transient) analysis of layered anisotropic composite-material plates. *Int. J. numer. Meth. Engng* **19**, 237–255 (1983).
4. J. N. Reddy and N. S. Putcha, Dynamic response of composite plates by a 3-D element, in *Recent Advances in Engineering Mechanics and their Impact on Civil Engineering Practice* (Edited by W. F. Chen and A. D. M. Lewis). ASCE Publication (1983).
5. J. N. Reddy, Geometrically nonlinear transient analysis of laminated composite plates. *AIAA J.* **21**, 621–629 (1983).
6. T. Kant and Mallikarjuna, Impulse response of anisotropic composite plates with a higher-order theory and finite element discretisation. Trans. 10th Int. Conf. on Structural Mechanics in Reactor Technology, Anaheim, U.S.A. (14–18 August 1989).
7. Mallikarjuna, Refined theories with  $C^0$  finite elements for free vibration and transient dynamics of anisotropic composite and sandwich plates. Ph.D. Dissertation, Department of Civil Engineering, Indian Institute of Technology, Bombay, India (1989).
8. J. K. Chen and C. T. Sun, Dynamic large deflection response of composite laminates subjected to impact. *Compos. Struct.* **4**, 59–73 (1985).
9. J. K. Chen and C. T. Sun, Nonlinear transient responses of initially stressed composite plates. *Comput. Struct.* **21**, 513–520 (1985).
10. T. von Kármán, Festigkeitsprobleme in Maschinenbau, Encyklopadie der mathematischen Wissenschaften. Teubner, Leipzig, 4, Art. 27, p. 350 (1907–1914).
11. S. J. Medwadowski, A refined theory of elastic, orthotropic plates. *J. appl. Mech.* **25**, 437–443 (1958).
12. I. K. Ebcioğlu, A large deflection theory of anisotropic plates. *Ingenieur-Archiv* **33**, 396–403 (1964).
13. J. N. Reddy, A simple higher-order theory for laminated composite plates. *J. appl. Mech.* **51**, 745–752 (1984).
14. J. N. Reddy, A refined nonlinear theory of plates with transverse shear deformation. *Int. J. Solids Struct.* **20**, 881–896 (1984).
15. N. S. Putcha and J. N. Reddy, A mixed shear flexible finite element for the analysis of laminated plates. *Comput. Meth. appl. Mech. Engng* **44**, 213–227 (1984).
16. J. N. Reddy, A review of the literature on finite-element modelling of laminated composite plates. *Shock Vib. Dig.* **17**, 3–8 (1985).
17. Mallikarjuna and T. Kant, Dynamics of laminated composite plates with a higher-order theory and finite element discretization. *J. Sound Vib.* **126**, 463–475 (1988).
18. Mallikarjuna and T. Kant, Free vibration of symmetrically laminated plates using a higher-order theory with finite element technique. *Int. J. numer. Meth. Engng* **29**, 1875–1889 (1989).
19. T. Kant and Mallikarjuna, A higher-order theory for free vibration of unsymmetrically laminated composite and sandwich plates—finite element evaluations. *Comput. Struct.* **32**, 1125–1132 (1989).
20. T. Kant and Mallikarjuna, Vibrations of unsymmetrically laminated plates using a higher-order theory and a  $C^0$  finite element formulation. *J. Sound Vib.* **134**, 1–16 (1989).
21. E. Hinton, T. A. Rock and O. C. Zienkiewicz, A note on mass lumping and related processes in the finite element method. *Earth Engng Struct. Dyn.* **4**, 245–249 (1976).
22. S. H. Yang and C. T. Sun, *Indentation Law for Composite Laminates* (Edited by I. M. Daniel), *ASTM STP 787*, 425–49 (1982).
23. T. M. Tan and C. T. Sun, Wave propagation in graphite/epoxy laminates due to Impact. NASA CR-168057 (December 1982).
24. D. R. J. Owen and E. Hinton, *Finite Elements in Plasticity—Theory and Practice*. Pineridge Press, Swansea, U.K. (1980).
25. T. Y. Tsui and P. Tong, Stability of transient solution of moderately thick plates by finite difference methods. *AIAA J.* **9**, 2062–3 (1971).
26. H. U. Akay, Dynamic large deflection analysis of plates using mixed finite elements. *Comput. Struct.* **11**, 1–11 (1980).
27. D. J. Bayles, R. L. Lowery and D. E. Bovd, Nonlinear vibrations of rectangular plates. *ASCE J. Struct. Div.* **99**, ST5 (1973).
28. N. Yamaki, Influence of large amplitude on flexural vibrations of elastic plates. *Zeitschrift fur Angewandte Mathematic und Mechanik* **41**, 501–510 (1961).
29. C. Y. Chia, *Nonlinear Analysis of Plates*. McGraw-Hill, New York (1980).
30. J. N. Reddy, *An Introduction to the Finite Element Method*. McGraw-Hill, New York (1985).